Electric field-assisted flash sintering of tin dioxide

R. Muccillo *, E.N.S. Muccillo *

Center of Science and Technology of Materials, Energy and Nuclear Research Institute, Travessa R 400, Cidade Universitária, S. Paulo, SP 05508-900, Brazil

Abstract

SnO$_2$ green pellets were submitted to ac electric fields at temperatures below 1350 °C. Electric current pulses occurred and a substantial modification was found in the microstructure of the pellets after application of 80 V cm^{-1} at 900, 1100 and 1300 °C. Similar experiments were carried out in SnO$_2$ mixed to 2 wt.% MnO$_2$. The linear shrinkage of the pellets was monitored with a dilatometer during the application of the electric field. Scanning electron microscopy micrographs of the pellets show the grain structure evolution after the electric current pulses. The larger is the electric current flow through the SnO$_2$ pellet, the larger are the shrinkage and the average grain size. Even though sintering occurs without significant densification in SnO$_2$, the welding of the grains is evident. The apparent density of green pellets of SnO$_2$ with MnO$_2$ addition sintered at 1100 °C increased 110% with the application of 80 V cm^{-1}, 5 A.
© 2013 Elsevier Ltd. All rights reserved.

Keywords: Flash sintering; Tin dioxide

1. Introduction

Tin oxide is an n-type semiconductor with application in many devices such as chemical sensors,[1–3] solar cells, displays and batteries.[4–6] Pure SnO$_2$ does not densify upon heating because of the predominance of the evaporation–condensation mechanism.[7] For sintering SnO$_2$ bulk ceramics from powders, sintering aids are required for avoiding the decomposition of SnO$_2$ to SnO at temperatures higher than 1300 °C.[8–10] The relative densities of a SnO$_2$ green pellet and of pellets sintered at 1000, 1100, 1220 and 1300 °C were reported as 49.8, 49.8, 49.9, 49.7 and 49.8%, respectively.[7] It is a common practice the mixing of sintering aids to achieve dense SnO$_2$, for example by liquid phase sintering with the addition of Li$_2$CO$_3$ or CuO.[7,10] Aliovalent cations have been proposed to form solid solutions, creating lattice defects and thereby promoting densification upon sintering by solid state diffusion.[8,10] Relative densities of 95% of the theoretical density and even higher values were obtained upon sintering SnO$_2$ with MnO$_2$ addition for a Mn/(Mn+Sn)$_{atomic}$ cation ratio equal to 4×10^{-3}.[11–13]

One of the more important recent developments on sintering ceramic materials involves the application of an electric field on heating a green pellet without applying pressure. The first reports on this new sintering technique showed that either dc or ac electric fields inhibited grain growth.[14,15] In ionic conducting ceramics, low dc electric fields were found to enhance the sintering rate and the plastic deformation.[16] Afterwards larger electric fields (>40 V cm^{-1}) were applied with significant densification in few seconds of Y-TZP[17] and Y-FSZ[18,19] at temperatures lower than 1000 °C. Flash sintering has been applied recently to many green pellets of different electrical behavior: alumina insulator,[20] Co$_2$MnO$_4$ electronic conductor,[21] cubic and tetragonal yttria-stabilized zirconia ionic conductors,[22–26] strontium-doped barium cerate protonic conductor,[27] ceria ionic conductor,[28] strontium titanate semiconductor[29] and polymorphic silicon carbide semiconductor.[30] Theoretical aspects (mechanism and grain growth) have also been reported.[22,24,31,32] Most of the experiments, independent on the attributed physical mechanism, reach the same general feature: the application of a dc or ac electric field with suitable magnitude promotes densification during sintering at temperatures which depend on the studied compound, but is always lower than the conventional sintering temperature. Recently the welding of the grains in yttria-stabilized zirconia was proposed to occur when an ac field is applied to these ceramics in the electrolytic region, namely, in

* Corresponding authors. Tel.: +55 11 31339203; fax: +55 11 31339276.
E-mail addresses: muccillo@usp.br (R. Muccillo), enavarro@usp.br (E.N.S. Muccillo).

the ionic conduction regime.[18] The welding of the grains happens in a singular current pulse (few seconds' half-width) and was ascribed to an intense Joule heating by the flow of an electric current through the inter-particle region of the green pellet. The increase in the inter-particle temperature might also promote densification and grain growth due to heat transfer to the bulk of the particles. This welding promotes a large decrease in the intergranular blocking of charge carriers, seen as a large reduction of the impedance spectroscopy arc at low frequencies, which represents the electrical resistivity of the grain boundaries. Even though Joule heating might occur, a full explanation of the mechanisms responsible for flash sintering and/or flash grain welding is still lacking.[22,24,31–33] Experiments were reported of flash sintering under constant electric fields or current densities,[34] with materials with different average particle sizes,[35] under continuous application of an electric field during heating and on the effects of the applied field and temperature on the incubation time for flash sintering,[36] and on application of very high electric fields.[37] This method of sintering has been applied with success to dog bone shape, cylindrical shape and tape-casted ceramics.[38] Few works deal with technological application of this sintering method, specifically for solid oxide fuel cells.[19,21,39,40]

Here we have to point out the main difference between flash sintering and flash grain welding: during a flash sintering experiment, either a dc or an ac field is applied; during a flash grain welding experiment, on the other hand, only an ac field is applied through the specimen, to promote charge but not mass transfer. Application of ac fields avoids depletion of ionic species inhibiting stoichiometry deviation, which produces, for example, the blackening effect in zirconia.[41–43] In ceramic materials with poor sinterability, like Gd-doped $BaCeO_3$, the application of an ac electric field promoted negligible changes in densification, although the grain boundary conductivity substantially improved.[27] That result along with those measured in granules of yttria-stabilized zirconia[25] show that the primary effect upon application of an ac electric field on an ionic conductor is the welding of the interfaces. In spite of the recognized success of this novel sintering technique, some important questions remain unanswered. It seems that the application of this technique to ceramic materials with poor sinterability like pure alumina[20] and silicon carbide[30] *without* sintering aids exerts minor effects on both microstructure and densification.

In this work, the effects of an ac electric field on sintering SnO_2 and SnO_2 mixed to MnO_2 were investigated at temperatures below the decomposition temperature of SnO_2.

2. Experimental

Tin (IV) oxide and manganese (IV) oxide from Alfa Aesar (99%) were used. The purity of the tin oxide powder was ascertained by X-ray fluorescence analysis (Shimadzu EDX-720) and the distribution of particle size was evaluated by laser scattering in a Cilas granulometer. SnO_2: 2 wt.% MnO_2 was prepared by thoroughly mixing and homogenization in an agate mortar. The SnO_2 and the SnO_2: 2 wt.% MnO_2 powders were uniaxially cold-pressed in ϕ 5 mm × 5–7 mm thickness at 30 MPa with

steel dies and isostatically at 200 MPa. The structural phase was determined by X-ray diffraction measurements in a Bruker-AXS model D8 Advance X-ray diffractometer with Cukα radiation (40 kV, 40 mA), 20–80° 2θ range, 0.05° step size, 3 s per step. For crystallite size evaluation using Scherrer equation,[44] the measurements were performed in the 51–53° 2θ range, which corresponds to the (2 1 1) reflection of SnO_2 (JCPDS 41-1445), 0.01° step size, 10 s per step.

The microstructure of fracture pellet surfaces, without any coating, was examined in a field emission gun scanning electron microscope (FEG-SEM FEI Inspect F50). Density was determined by measuring the weight and dimensions of the compact before and after sintering. The theoretical density (TD) was considered to be 6.993 g cm^{-3}.[8]

The experimental setup for simultaneously applying ac/dc voltage and monitoring shrinkage was described elsewhere.[26] Briefly, it consists in a vertical dilatometer (0.5 μm precision) with Pt electrical connections from both flat surfaces of cylindrical pellets to a homemade 30–60 V, 1–10 A ac power supply operating in the frequency range 500–1000 Hz. The applied electric voltage turns off when the electric current reaches a pre-set value in the 1–10 A range. Multiple electric current pulses may be applied by turning on the applied voltage. The shrinkage of the specimen is monitored in the dilatometer and the voltage–current data is collected in a pc-controlled homemade data logger. Sintering has been carried out at 900, 1100 and 1300 °C dilatometer temperatures without and with 80–100 V cm^{-1} (1 kHz) pulses with the electric current limited either to 1 A or 5 A.

3. Results and discussion

The analysis of the distribution of particle size of the commercial SnO_2 powders, which purity was determined as 98.6% by fluorescence X-ray analysis, shows that it is composed primordially of agglomerated particles with approximately 1 μm average size. The average crystallite size, estimated by X-ray diffraction was 373 nm.

3.1. SnO_2

Fig. 1a–c shows dilatometric curves of SnO_2 green pellets exposed to 5 min sequential electric current pulses at temperatures close to 900 °C, 1100 °C and 1300 °C, respectively. In the figures, the dilatometric curves of samples just heated and cooled in the dilatometer without the application of an ac field are also shown. Shrinkage due to the application of the electric field is evident. Heating the green SnO_2 pellet to 900 °C produces no appreciable densification (44.5%TD, green density 41.8%TD). The application of 80 V cm^{-1} with 1 A limiting current at ∼900 °C leads to negligible but measurable 5% longitudinal shrinkage. Just heating to a larger temperature, 1100 °C, produces an expected small shrinkage of 0.2% (45.2%TD), which changes to 5.6% upon the application of the electric field. A further 200 °C increase in the temperature to 1300 °C does not show substantial increment in shrinkage. The shrinkage limits attained were 5.0%, 5.6% and 5.8% at 900 °C, 1100 °C
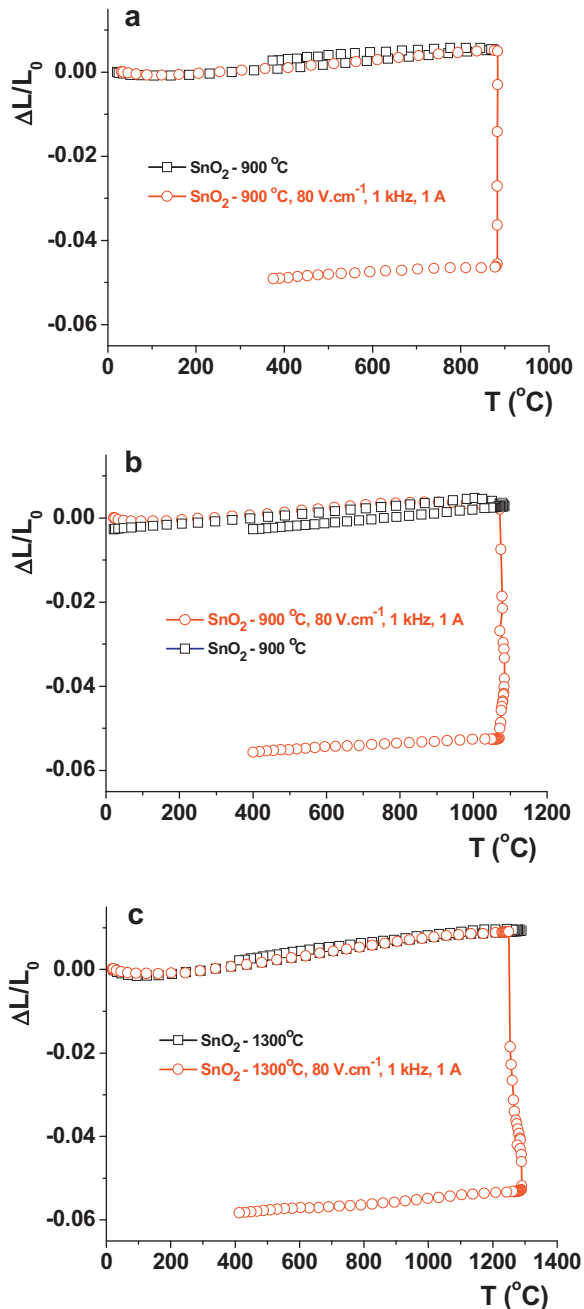
Fig. 1. Dilatometric curves of SnO_2 without and with (flash sintering) application of $80\,V\,cm^{-1}$ (1 kHz, 1 A limiting current) at 900 °C (a), 1100 °C (b) and 1300 °C (c).
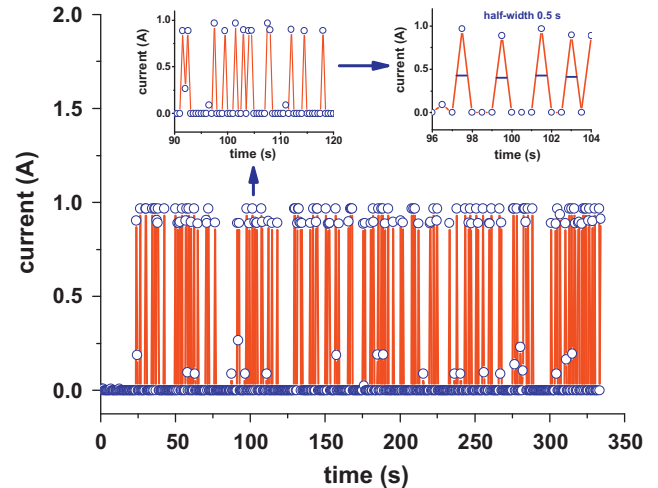

Fig. 2. Typical electrical current pulses on SnO_2 for 1 A limiting current. The insets are exploded views of parts of the current × time plot. Top right inset indicates 0.5 s single pulse half-width.

may consider that in the case of zirconia-yttria, the flash sintering occurs in the high temperature extreme of the electrolytic window, with oxide ions being the major charge carriers. In the case of tin oxide, on the other hand, the charge carriers are electrons, which are expected to produce lower Joule heating than O^{2-} ions under 1 kHz applied electric field. Enough heat is released to the grains welding them, and consequently inhibiting the passage of electric currents, i.e., stopping the pulses.

Another series of dilatometric experiments has been carried out by changing the maximum current allowed to cross the specimen during the application of the ac electric field. The results for pulses at 900 °C with limitation of electric current to 1 A and to 5 A are shown in Fig. 3, together with the shrinkage monitoring without voltage application to the specimen. As expected, the larger is the available current through the specimen, the larger is the delivered power (Joule heating is proportional to the square of the current) and consequently, the larger is the shrinkage level (from 5 to 11%). This is an evidence that limiting the electrical current through the specimen is a key issue to the final retraction of the green pellet and, consequently, to its densification.

The microstructure of the pellets submitted to the application of ac electric fields was observed by scanning electron
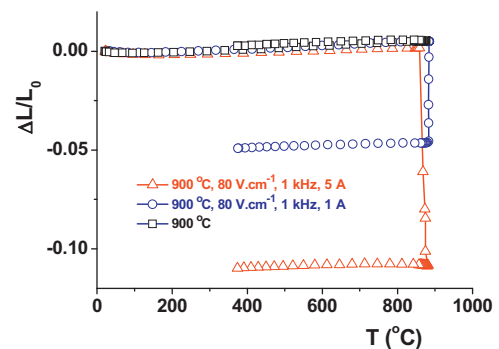
and 1300 °C, respectively, for $80\,V\,cm^{-1}$, 1 kHz, 1 A maximum current.

Fig. 2 shows typical profiles of the 1 A limited electric current sequential pulses caused by the application of $80\,V\,cm^{-1}$, 1 kHz, through the SnO_2 specimens. A large number of pulses, each one with approximately 0.5 s half-width, are required for achieving a maximum shrinkage level at each temperature. This is a quite different behavior from what happens in the case of applying ac fields to zirconia-yttria ionic conductors[18,26] and barium cerate proton conductor,[27] where a single pulse was sufficient for sintering. The reason for that is not clear yet, but one

Fig. 3. Dilatometric results of SnO_2 from room temperature to 900 °C without and with application of $80\,V\,cm^{-1}$ during 5 min, limiting the current to 1 A and to 5 A.
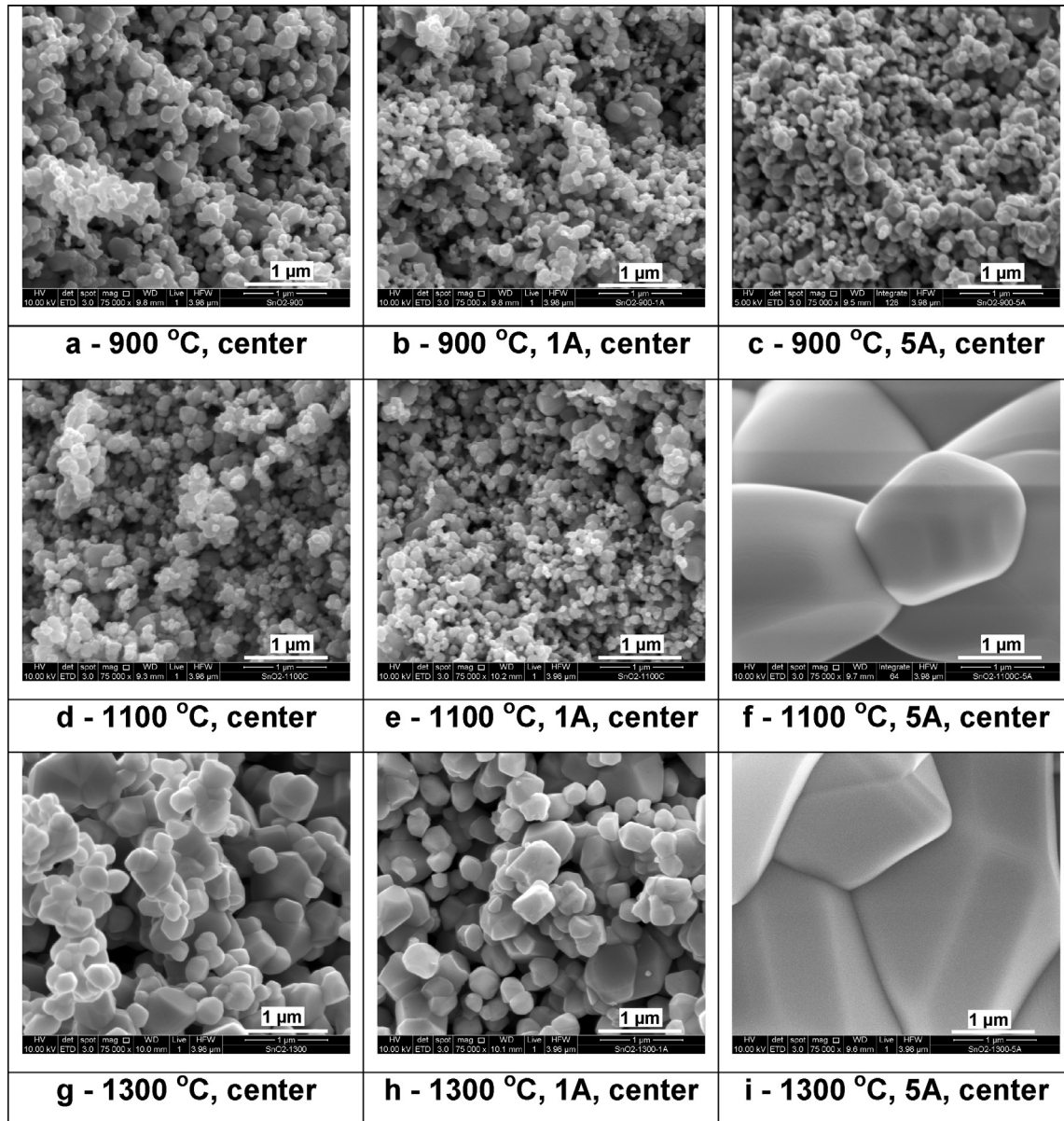
Fig. 4. Scanning electron microscopy micrographs of SnO_2 before and after exposure to $80\,V\,cm^{-1}$ at $900\,°C$ (a–c), $1100\,°C$ (d–f) and $1300\,°C$ (g–i). Limiting current: 1 A (b, e, h); 5 A (c, f, i). *Images taken at the top fracture **center** of the samples.*

microscopy on diametric fracture surfaces of the specimens. Observations were focused in the central part of the fracture surfaces and near the border. The reason is that we noticed, as also reported recently for SiC,[30] that the density decreases from the center toward the border in flash sintered samples. This might be due to the preferential path of the charged species longitudinally through the center of the samples, which gets hot by the delivered Joule heating and then irradiates to the borders. This preferential path is explained by the relatively low green density and non-homogeneity of the packed particles in the bulk of the samples being heated from the outside by the heating elements of the furnace. The results are shown in Figs. 4 (center) and 5 (border) for the SnO_2 samples.

Fig. 4 shows FEG-SEM micrographs with the same magnitude and scale bars of the microstructure of the *center* of

SnO_2 not flash-sintered (Fig. 4a, d, g) and flash sintered at $900\,°C$, $1100\,°C$ and $1300\,°C$ with 1 A (Fig. 4b, e, h) and 5 A (Fig. 4c, f, i) limiting current, respectively. The micrograph of the sample after application of the ac electric field with 1 A limiting current at $900\,°C$, which promotes a negligible 5.0% shrinkage (Fig. 4b), is similar to the micrograph of the non-flash-sintered sample (Fig. 4a). It consists of a large portion of submicron grains and relatively few large grains. This means that pressing and heating SnO_2 powders lead to multimodal grain growth and the subsequent application of an ac electric field with a relatively low limiting current does not improve the densification or the microstructure. A similar effect is observed by applying a 5 times larger limiting current, while keeping the magnitude of the electric field: the shrinkage level reaches 11% and the micrograph exhibits a large increase in
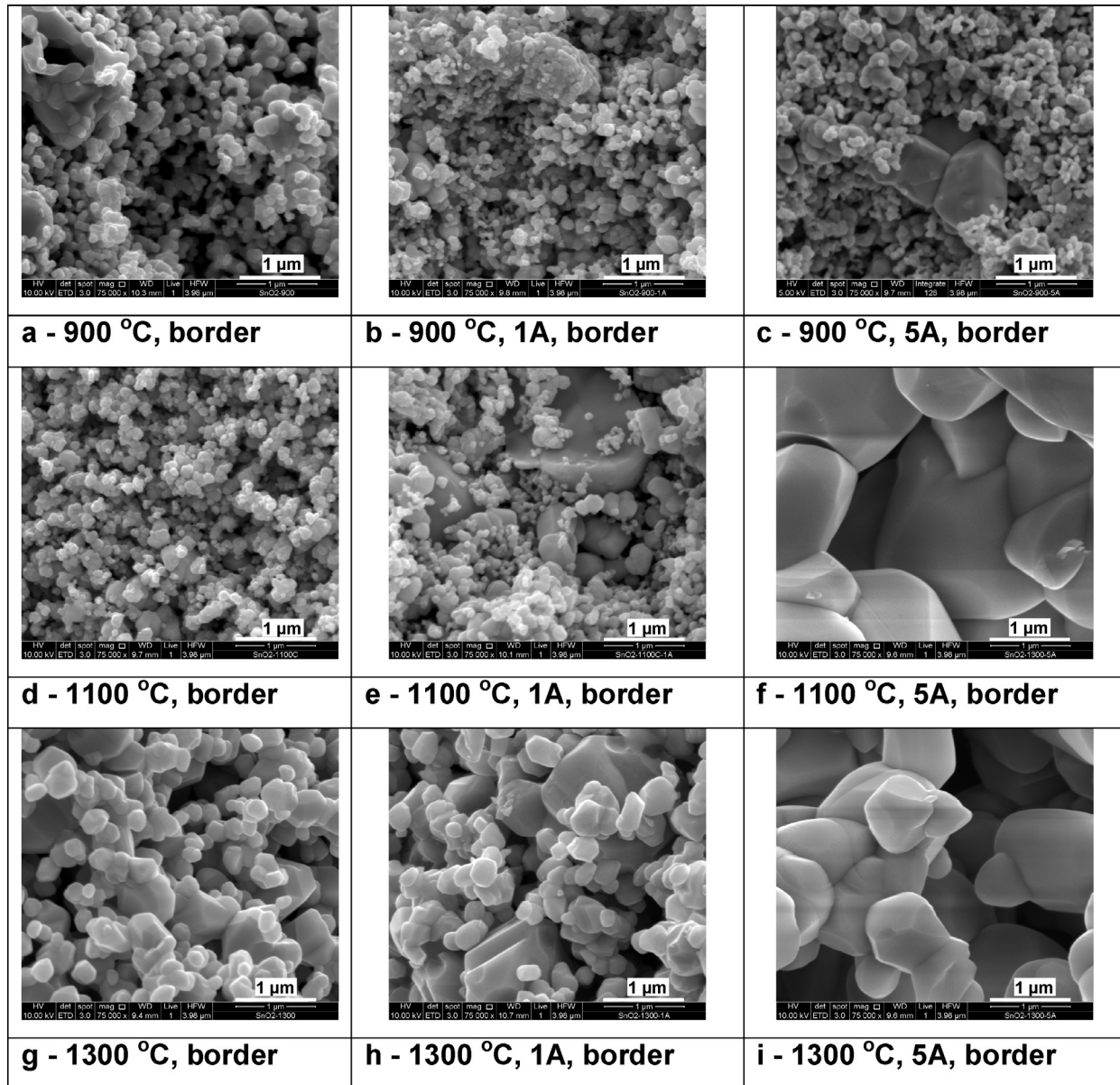
Fig. 5. Scanning electron microscopy micrographs of SnO_2 before and after exposure to 80 V cm^{-1} at 900 °C (a–c), 1100 °C (d–f) and 1300 °C (g–i). Limiting current: 1 A (b, e, h); 5 A (c, f, i). *Images taken at the top fracture **border** of the samples.*

the average grain size (Fig. 4c). After heating to 900 °C, all specimens exhibit a wide distribution of grain sizes. The specimens still show very large as well as relatively very small grains. After increasing the temperature by only 200°, the situation is identical for the blank specimen (no flash-sintering, Fig. 4d) and for the specimen exposed to 1 A limiting current pulses (Fig. 4e), while the specimen with a 5-fold increase of the limiting current has relatively very large grains welded together (Fig. 4f). This is a typical example of flash grain welding. A similar reasoning may be proposed for the analysis of the micrographs acquired after further 200 °C increase in the temperature (Fig. 4g–i).

Fig. 5 shows FEG-SEM micrographs, with the same magnitude and scale bars, near the *border* of SnO_2 not flash

sintered (Fig. 5a, d, g) and flash sintered at 900 °C, 1100 °C and 1300 °C with 1 A (Fig. 5b, e, h) and 5 A (Fig. 5c, f, i) limiting current, respectively. A comparison of the micrographs of SnO_2 samples sintered without the application of electric field (Figs. 4a and 5a, 4d and 5d, 4g and 5g for 900 °C, 1100 °C and 1300 °C, respectively) shows similar features anywhere at the fracture surface. The micrographs of the fracture surfaces of flash sintered SnO_2 samples, on the other hand, show evident differences when one compares the micrographs taken at the center and near the border. The differences are more evident in Figs. 4i and 5i for 5 A limited current at 1300 °C. The average grain sizes are larger at the center than near the border. Further research work is required to understand and eventually circumvent this problem to produce homogeneous specimens.
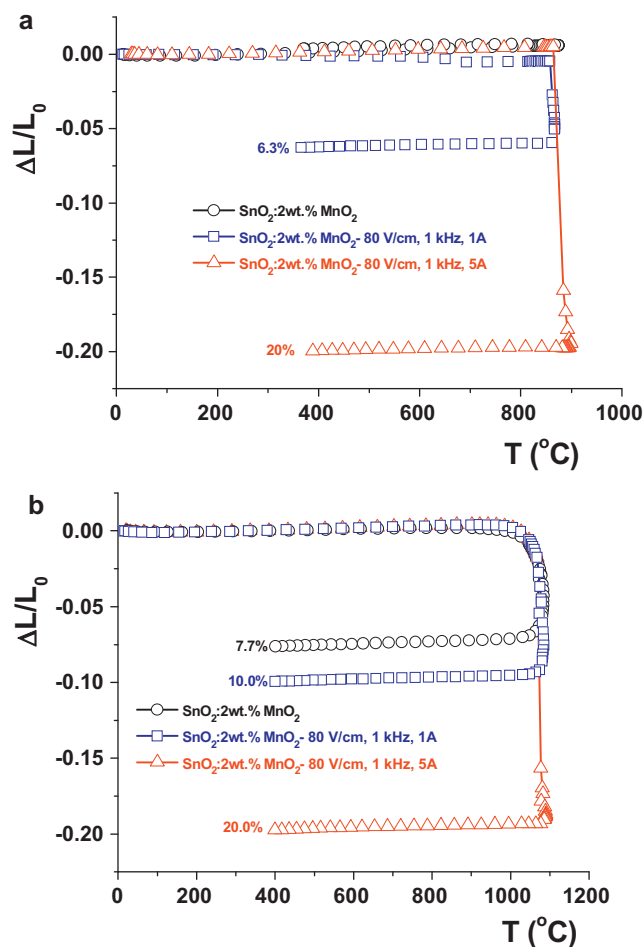
Fig. 6. Dilatometric results of SnO_2 and $SnO_2 + 2$ wt.% MnO_2 from room temperature to 900 °C (a) and to 1100 °C (b) with application of 80 V cm^{-1} during 5 min, limiting the current to 1 A and to 5 A.

3.2. SnO_2 mixed to MnO_2

Another experiment was designed to take into account the role of divalent impurities during sintering SnO_2, which have been reported as sintering aids.[7–12] Fig. 6 shows the evaluation of the shrinkage profile during flash sintering SnO_2 and SnO_2 with addition of 2 wt.% MnO_2 under the same conditions at 900 °C (Fig. 6a) and 1100 °C (Fig. 6b). The results show that MnO_2 acts effectively as a sintering aid. The achieved final shrinkage levels at 900 °C are 6.3% and 20.0% for 1 A and 5 A limiting current, respectively. However, at 1100 °C these values are 10.0% and 20.0%. The final shrinkage level for a 5 A limiting current does not depend on the temperature, probably because 20.0% shrinkage is a threshold level for this experimental conditions and there are no more available paths for the electric current flow through the biased specimen. The addition of manganese dioxide to tin dioxide does not improve densification after heating to 900 °C and even to 1100 °C (only 7.7% linear shrinkage).

Fig. 7 shows FEG-SEM micrographs collected at the center and near the border of SnO_2 mixed to 2 wt.% MnO_2 sintered at 900 °C (Fig. 7a and b) and after the application of ac electric voltages at 900 °C with 1 A (Fig. 7c and d) and 5 A (Fig. 7e

Table 1
Average crystallite size of conventionally and flash sintered SnO_2 and SnO_2+2% MnO_2 specimens at 900 °C.

Specimen	Flash electrical current (A)	Average crystallite size (nm)
SnO_2	–	373
SnO_2	5.0	722
$SnO_2 + 2\%MnO_2$	–	527
$SnO_2 + 2\%MnO_2$	5.0	757

and f) limiting currents. A comparison with the micrographs of specimens without MnO_2 addition shows that the average grain sizes reach lower values. This means that MnO_2 is not only a densification agent, but also a grain growth inhibitor.

Fig. 8 shows FEG-SEM micrographs of $SnO_2 + 2$ wt.% MnO_2 heated up to 900 °C without and with the application of 80 V cm^{-1} with a limiting current of 5 A. The morphology of the grains is similar to the one observed in SnO_2 without MnO_2 addition. The sample submitted to multiple 5 A current pulses shows larger grains. Residual pores are localized at the triple junctions and the grains are of polygonal shape with well defined edges.

The apparent densities of some specimens with manganese dioxide addition non-flashed and flash sintered with 1 A and 5 A limiting current show that there is a significant contribution of the electric field to the increase in the final density. For example, applying 80 V cm^{-1} with 5 A limiting current at 900 °C increases the density from 55.3% to 84.0%. At 1100 °C, the increase is from 66.3% to 91.8%.

X-ray diffraction measurements of all SnO_2 specimens with and without MnO_2 addition, sintered either with or without applying electric voltage, showed only the tetragonal crystalline structure of SnO_2 (JCPDF pattern 41-1445). Interesting features, shown in Table 1, were observed after the evaluation of the mean crystallite size using the Scherrer equation applied to the (2 1 1) reflection. The application of the ac electric field with a 5 A limited current in the SnO_2 sample promoted a 94% increase of the crystallite size. In the sample with MnO_2 addition, the increase was 44%, but >100% in comparison with the pure sample. The main implication of these figures is that Joule heating is indeed acting, delivering heat and increasing the crystallite size. Even though the X-ray diffraction patterns did not reveal SnO_2 reduction to SnO or to metallic Sn, black dots were clearly observed in the FEG-SEM micrographs of specimens exposed to 5 A current flashes, meaning that through some preferential paths the increase in the local temperature was such that total reduction of SnO_2 might have occurred.

4. Summary

4.1. SnO_2 without sintering aid

- The effect of the ac electric field is to promote limited linear shrinkage, associated to the welding of the grains without significant densification.
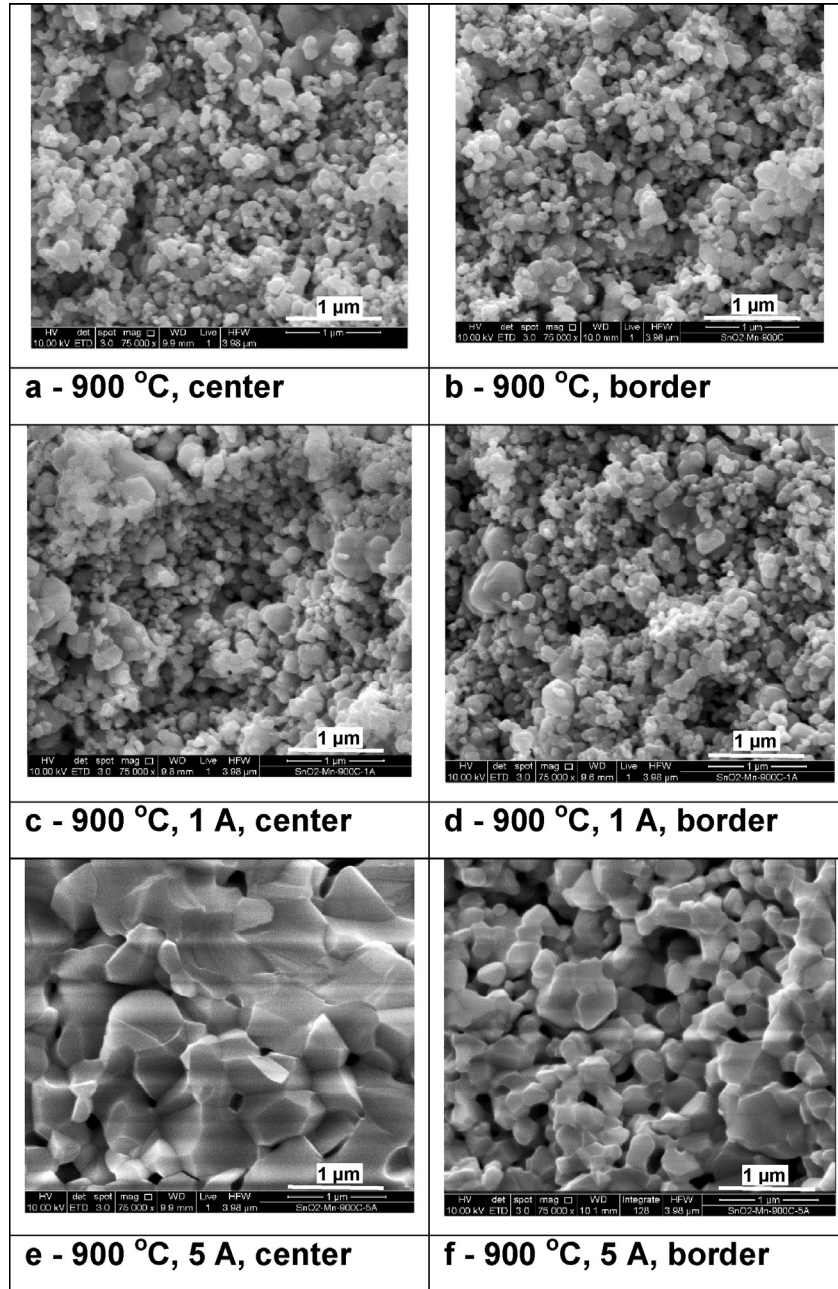
a - 900 °C, center

b - 900 °C, border

c - 900 °C, 1 A, center

d - 900 °C, 1 A, border

e - 900 °C, 5 A, center

f - 900 °C, 5 A, border

Fig. 7. Scanning electron microscopy micrographs of fracture surfaces of $SnO_2 + 2$ wt.% MnO_2: (a) and (b) sintered at 900 °C; (c) and (d) after exposure for 5 min to 80 V cm^{-1}, 1 kHz, 1 A limiting current at 900 °C; (e) and (f) after exposure to 80 V cm^{-1}, 1 kHz, 5 A limiting current at 900 °C.
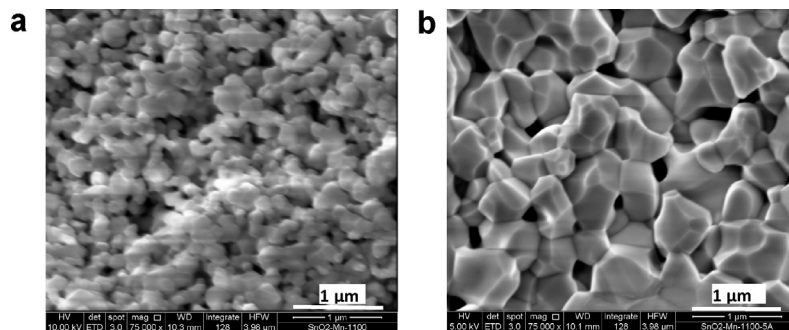

Fig. 8. Scanning electron microscopy micrographs of SnO_2 mixed to 2 wt.% SnO_2 heated up to 1100 °C (a) and after exposure for 5 min to 80 V cm^{-1}, 1 kHz, 5 A limiting current at 1100 °C.

- The average grain size increases for increasing the limiting current for temperatures higher than 900 °C. The average grain size is larger at the center than near the border.

4.2. SnO₂ with sintering aid (manganese dioxide)

- The linear shrinkage is negligible in specimens heated to 900 °C without the application of the ac electric field, in agreement with reports that sintering tin dioxide with sintering aids happens only at temperatures higher than 1000 °C.[12] The application of an ac electric field at that temperature promotes 6.0% and 20% shrinkages for 1 A and 5 A limiting currents, respectively, meaning that the main effect of the electric field is to enhance densification. This is the first time this experimental evidence is shown for SnO₂.
- The increase of the limiting current improves densification and increases the average grain size in tin dioxide. In yttria-stabilized zirconia, an ionic conductor, grain growth was shown to be inhibited upon flash sintering.
- The black spots observed in the FEG-SEM micrographs of specimens after 5 A current pulses are an indication that Joule heating might be predominant during the current pulses, with drastic increase of the local temperature.

5. Conclusions

Pure commercial SnO₂ powders, pressed to green pellets, were for the first time subjected to ac electric fields to evaluate the possibility of densification by flash sintering. Similar to what happens after conventional sintering, this compound does not reach significant densification, even though 11% shrinkage is attained at 900 °C under 80 V cm⁻¹. The amplitude of the electric current generated at the sample during the application of the electric field is found to be a key factor for welding grains and promoting grain growth. Considering that the larger is the limiting current, the larger is the Joule heating delivered to the intergranular regions of tin oxide, the larger is the average grain size, as observed in the FEG-SEM micrographs. These micrographs show that under flash sintering there is a huge and abnormal grain growth, the grains sticking together (flash grain welding) but preserving the pore structure that inhibits densification. The exaggerated grain growth suggests that besides the non-densifying evaporation–condensation mechanism, another mechanism plays a role during electric-field assisted sintering. However, sintering with densification (94%TD) has been achieved at a temperature 400 °C lower than the conventional one, by adding manganese dioxide to tin oxide. This is the first report such a high density is obtained for tin dioxide at temperatures below 1000 °C, an evidence that the application of electric fields improves its densification.

Acknowledgements

References

1. Ponce MA, Malagu C, Carotta MC, Martinelli G, Aldao CM. Gas inter-diffusion contribution to impedance in tin oxide thick films. *J Appl Phys* 2008;**104**:054907.
2. Batzill m, Diebold U. The surface and materials science of tin oxide. *Prog Surf Sci* 2005;**79**:47–154.
3. Kim Il-Doo, Rothschild A, Tuller HL. Advances and new directions in gas-sensing devices. *Acta Mater* 2013;**61**:974–1000.
4. Lewis BG, Paine DC. Applications and processing of transparent conducting oxides. *MRS Bull* 2000;**25**:22–7.
5. Maddalena A, Maschio RD, Dire S, Raccanelli A. Electrical conductivity of tin oxide films prepared by the sol–gel technique. *J Non-Cryst Solids* 1990;**121**: 365–9.
6. Kim SS, Choi SY, Park CG, Jin HW. Transparent conductive ITO thin films through the sol–gel process using molten salts. *Thin Solid Films* 1999;**347**:155–60.
7. Dolet N, Heintz JM, Rabardel L, Onillon M, Bonnet JP. Sintering mechanism of 0.99 SnO₂–0.01 CuO mixtures. *J Mater Sci* 1995;**30**:365–8.
8. Kimura T, Inada S, Yamaguchi T. Microstructure development in SnO₂ with and without additives. *J Mater Sci* 1989;**24**:220–6.
9. Takahashi J, Yamai I, Saito H. Effect of Nb₂O₅ on the Sintering of SnO₂. *J Ceram Soc Jpn* 1975;**83**:362–6.
10. Paria MK, Basu S, Paul A. Enhanced sintering of tin oxide with additives under isothermal conditions. *Trans Ind Ceram Soc* 1983;**42**:90–5.
11. Gouvea D, Varela JA, Smith A, Bonnet JP. Morphological characteristics of SnO₂ based powders containing manganese. *Eur J Solid State Inorg Chem* 1996;**33**:343–54.
12. Cerri JA, Leite ER, Gouvea D, Longo E, Varela JA. Effect of cobalt(II) oxide and manganese(IV) oxide on sintering of tin(IV) oxide. *J Am Ceram Soc* 1996;**79**:799–804.
13. Gouvea D, Smith A, Bonnet JP, Varela JA. Densification and coarsening of SnO₂-based materials containing manganese oxide. *J Eur Ceram Soc* 1998;**18**:345–51.
14. Yang D, Conrad H. Enhanced sintering rate of zirconia (3Y-TZP) by application of a small AC electric field. *Scripta Mater* 2010;**63**: 328–31.
15. Yang D, Raj R, Conrad H. Enhanced sintering rate of zirconia (3Y-TZP) through the effect of a weak dc electric field on grain growth. *J Am Ceram Soc* 2010;**93**:2935–7.
16. Ghosh S, Chokshi AH, Lee P, Raj R. A huge effect of weak dc electrical fields on grain growth in zirconia. *J Am Ceram Soc* 2009;**92**:1856–9.
17. Cologna M, Rashkova B, Raj R. Flash sintering of nanograin zirconia in <5 s at 850°C. *J Am Ceram Soc* 2010;**93**:3556–9.
18. Muccillo R, Kleitz M, Muccillo ENS. Flash grain welding in yttria stabilized zirconia. *J Eur Ceram Soc* 2011;**31**:1517–21.
19. Cologna M, Prette ALG, Raj R. Flash-sintering of cubic yttria-stabilized zirconia at 750°C for possible use in SOFC manufacturing. *J Am Ceram Soc* 2011;**94**:316–9.
20. Cologna M, Francis JSC, Raj R. Field assisted and flash sintering of alumina and its relationship to conductivity and MgO-doping. *J Eur Ceram Soc* 2011;**31**:2827–37.
21. Prette ALG, Cologna M, Sglavo VM, Raj R. Flash sintering of Co₂MnO₄ spinel for solid oxide fuel cell applications. *J Power Sources* 2011;**196**:2061–5.
22. Grasso S, Sakka Y, Rendtorff N, Hu C, Maizza G, Borodianska H, et al. Modeling of the temperature distribution of flash sintered zirconia. *J Ceram Soc Jpn* 2011;**119**:144–6.
23. Raj R, Cologna M, Francis JSC. Influence of externally imposed and internally generated electrical fields on grain growth, diffusional creep, sintering and related phenomena in ceramics. *J Am Ceram Soc* 2011;**94**:1941–65.
24. Baraki R, Schwarz S, Guillon O. Effect of electrical field/current on sintering of fully stabilized zirconia. *J Am Ceram Soc* 2012;**95**:75–8.
25. Cordier A, Kleitz M, Steil MC. Welding of yttrium-doped zirconia granules by electric current activated sintering (ECAS): protusion formation as a possible intermediate step in the consolidation mechanism. *J Eur Ceram Soc* 2012;**32**:1473–9.

26. Muccillo R, Muccillo ENS. An experimental setup for shrinkage evaluation during electric field-assisted flash sintering: application to yttria-stabilized zirconia. *J Eur Ceram Soc* 2013;**33**:515–20.

27. Muccillo R, Muccillo ENS, Kleitz M. Densification and enhancement of the grain boundary conductivity of gadolinium-doped barium cerate by ultra-fast flash grain welding. *J Eur Ceram Soc* 2012;**32**:2311–6.

28. Hao X, Liu Y, Wang Z, Qiao J, Sun K. A novel sintering method to obtain fully dense gadolinia doped ceria by applying a direct current. *J Power Sources* 2012;**210**:86–91.

29. Karakuscu A, Cologna M, Yarotski D, Won J, Francis JSC, Raj R, et al. Defect structure of flash-sintered strontium titanate. *J Am Ceram Soc* 2012;**95**:2531–6.

30. Zapata-Solvas E, Bonilla S, Wilshaw PR, Todd RI. Preliminary investigation of flash sintering of SiC. *J Eur Ceram Soc* 2013;**33**:2811–6.

31. Narayan J. Grain growth model for electric field-assisted processing and flash sintering of materials. *Scripta Mater* 2013;**68**:785–8.

32. Narayan J. A new mechanism for field-assisted processing and flash sintering of materials. *Scripta Mater* 2013;**69**:107–11.

33. Raj R. Joule heating during flash sintering. *J Eur Ceram Soc* 2012;**32**:2293–301.

34. Steil MC, Marinha D, Aman Y, Gomes JRC, Kleitz M. From conventional ac flash sintering of YSZ to hyper-flash and double flash. *J Eur Ceram Soc* 2013;**33**:2093–101.

35. Francis JSC, Cologna M, Raj R. Particle size effect in flash sintering. *J Eur Ceram Soc* 2012;**32**:3129–36.

36. Francis JSC, Raj R. Influence of the field and the current limit on flash sintering at isothermal furnace temperature. *J Am Ceram Soc* 2013;**96**:2754–8.

37. Downs JA, Sglavo VM. Electric field assisted sintering of cubic zirconia at 390°C. *J Am Ceram Soc* 2013;**96**:1342–4.

38. Akbari-Fakhrabadi A, Mangalaraja RV, Sanhueza FA, Avila RE, Ananthakumar S, Chan SH. Nanostructured Gd-CeO$_2$ electrolyte for solid oxide fuel cell by aqueous tape casting. *J Power Sources* 2012;**218**:307–12.

39. Liu Y, Hao X, Wang Z, Wang J, Qiao J, Yan Y, et al. A newly-developed effective direct current assisted sintering technique for electrolyte film densification of anode-supported solid oxide fuel cells. *J Power Sources* 2012;**215**:296–300.

40. Francis JSC, Cologna M, Montinaro D, Raj R. Flash sintering of anode-electrolyte multilayers for SOFC applications. *J Am Ceram Soc* 2013;**96**:1352–4.

41. Casselto RE, Penny J, Reynolds MJ. Structural consequences of blackening in yttria-stabilized zirconia. *Trans J Brit Ceram Soc* 1971;**70**, 115-&.

42. Moghadan FK, Yamashita T, Stevenson DA. Characterization of the current-blackening phenomena in scandia stabilized zirconia using transmission electron-microscopy. *J Mater Sci* 1983;**18**:2255–9.

43. Janek J, Korte C. Electrochemical blackening of yttria-stabilized zirconia – morphological instability of the moving reaction front. *Solid State Ionics* 1999;**116**:181–95.

44. Warren BE. *X-ray diffraction*. New York: Dover Publications, Inc.; 1990. p. 251.